

# Measurement of $\Gamma(\eta \rightarrow \pi^+\pi^-\gamma)/\Gamma(\eta \rightarrow \pi^+\pi^-\pi^0)$ with the KLOE Detector

The KLOE / KLOE-2 Collaboration

D. Babusci<sup>i</sup>, D. Badoni<sup>q,r</sup>, I. Balwierz-Pytko<sup>h</sup>, G. Bencivenni<sup>i</sup>,  
 C. Bini<sup>o,p</sup>, C. Bloise<sup>i</sup>, V. Bocci<sup>p</sup>, F. Bossi<sup>i</sup>, P. Branchini<sup>t</sup>,  
 A. Budano<sup>s,t</sup>, L. Caldeira Balkeståhl<sup>v</sup>, G. Capon<sup>i</sup>,  
 F. Ceradini<sup>s,t</sup>, P. Ciambrone<sup>i</sup>, E. Czerwiński<sup>i</sup>, E. Dané<sup>i</sup>,  
 E. De Lucia<sup>i</sup>, G. De Robertis<sup>b</sup>, A. De Santis<sup>o,p</sup>, P. De Simone<sup>i</sup>,  
 A. Di Domenico<sup>o,p</sup>, C. Di Donato<sup>l,\*</sup>, B. Di Micco<sup>s,t</sup>,  
 R. Di Salvo<sup>r</sup>, D. Domenici<sup>i</sup>, O. Erriquez<sup>a,b</sup>, G. Fanizzi<sup>a,b</sup>,  
 A. Fantini<sup>q,r</sup>, G. Felici<sup>i</sup>, S. Fiore<sup>o,p</sup>, P. Franzini<sup>o,p</sup>,  
 P. Gauzzi<sup>o,p</sup>, G. Giardina<sup>j,e</sup>, S. Giovannella<sup>i</sup>, F. Gonnella<sup>q,r</sup>,  
 E. Graziani<sup>t</sup>, F. Happacher<sup>i</sup>, B. Höistad<sup>v</sup>, L. Iafolla<sup>i</sup>,  
 M. Jacewicz<sup>v,\*</sup>, T. Johansson<sup>v</sup>, A. Kupsc<sup>v</sup>, J. Lee-Franzini<sup>i,u</sup>,  
 B. Leverington<sup>i</sup>, F. Loddo<sup>b</sup>, S. Loffredo<sup>s,t</sup>, G. Mandaglio<sup>j,e,d</sup>,  
 M. Martemianov<sup>k</sup>, M. Martini<sup>i,n</sup>, M. Mascolo<sup>q,r</sup>, R. Messi<sup>q,r</sup>,  
 S. Miscetti<sup>i</sup>, G. Morello<sup>i</sup>, D. Moricciani<sup>r</sup>, P. Moskal<sup>h</sup>,  
 F. Nguyen<sup>s,t</sup>, A. Passeri<sup>t</sup>, V. Patera<sup>m,i</sup>, I. Prado Longhi<sup>s,t</sup>,  
 A. Ranieri<sup>b</sup>, C. F. Redmer<sup>v</sup>, P. Santangelo<sup>i</sup>, I. Sarra<sup>i</sup>,  
 M. Schioppa<sup>f,g</sup>, B. Sciascia<sup>i</sup>, M. Silarski<sup>h</sup>, C. Taccini<sup>s,t</sup>,  
 L. Tortora<sup>t</sup>, G. Venanzoni<sup>i</sup>, R. Versaci<sup>i,x</sup>, W. Wiślicki<sup>w</sup>,  
 M. Wolke<sup>v</sup>, G. Xu<sup>i,c</sup>, J. Zdebik<sup>h</sup>

<sup>a</sup>*Dipartimento di Fisica dell'Università di Bari, Bari, Italy.*

<sup>b</sup>*INFN Sezione di Bari, Bari, Italy.*

<sup>c</sup>*Institute of High Energy Physics of Academica Sinica, Beijing, China.*

<sup>d</sup>*Centro Siciliano di Fisica Nucleare e Struttura della Materia, Catania, Italy.*

<sup>e</sup>*INFN Sezione di Catania, Catania, Italy.*

<sup>f</sup>*Dipartimento di Fisica dell'Università della Calabria, Cosenza, Italy.*

<sup>g</sup>*INFN Gruppo collegato di Cosenza, Cosenza, Italy.*

<sup>h</sup>*Institute of Physics, Jagiellonian University, Cracow, Poland.*

<sup>i</sup>*Laboratori Nazionali di Frascati dell'INFN, Frascati, Italy.*

<sup>j</sup>*Dipartimento di Fisica e Scienze della Terra dell'Università di Messina, Messina, Italy.*

<sup>k</sup>*Institute for Theoretical and Experimental Physics (ITEP), Moscow, Russia.*

<sup>l</sup>*INFN Sezione di Napoli, Napoli, Italy.*

<sup>m</sup>*Dipartimento di Scienze di Base ed Applicate per l'Ingegneria dell'Università "Sapienza", Roma, Italy.*

<sup>n</sup>*Dipartimento di Scienze e Tecnologie applicate, Università "Guglielmo Marconi", Roma, Italy.*

<sup>o</sup>*Dipartimento di Fisica dell'Università "Sapienza", Roma, Italy.*

<sup>p</sup>*INFN Sezione di Roma, Roma, Italy.*

<sup>q</sup>*Dipartimento di Fisica dell'Università "Tor Vergata", Roma, Italy.*

<sup>r</sup>*INFN Sezione di Roma Tor Vergata, Roma, Italy.*

<sup>s</sup>*Dipartimento di Fisica dell'Università "Roma Tre", Roma, Italy.*

<sup>t</sup>*INFN Sezione di Roma Tre, Roma, Italy.*

<sup>u</sup>*Physics Department, State University of New York at Stony Brook, USA.*

<sup>v</sup>*Department of Physics and Astronomy, Uppsala University, Uppsala, Sweden.*

<sup>w</sup>*National Centre for Nuclear Research, Warsaw, Poland.*

<sup>x</sup>*Present Address: CERN, CH-1211 Geneva 23, Switzerland.*

---

## Abstract

The ratio  $R_\eta = \Gamma(\eta \rightarrow \pi^+\pi^-\gamma)/\Gamma(\eta \rightarrow \pi^+\pi^-\pi^0)$  has been measured by analysing 22 million  $\phi \rightarrow \eta\gamma$  decays collected by the KLOE experiment at DAΦNE, corresponding to an integrated luminosity of 558 pb<sup>-1</sup>. The  $\eta \rightarrow \pi^+\pi^-\gamma$  proceeds both via the  $\rho$  resonant contribution, and possibly a non-resonant direct term, connected to the box anomaly. Our result,  $R_\eta = 0.1856 \pm 0.0005_{\text{stat}} \pm 0.0028_{\text{syst}}$ , points out a sizable contribution of the direct term to the total width. The di-pion invariant mass for the  $\eta \rightarrow \pi^+\pi^-\gamma$  decay could be described in a model-independent approach in terms of a single free parameter,  $\alpha$ . The determined value of the parameter  $\alpha$  is  $\alpha = (1.32 \pm 0.08_{\text{stat}}^{+0.10}_{-0.09_{\text{syst}}} \pm 0.02_{\text{theo}})$  GeV<sup>-2</sup>.

*Key words:*  $e^+e^-$  collisions,  $\eta$  decays, light mesons, chiral perturbation theory

---

---

\* Corresponding author.

*Email addresses:* [camilla.didonato@na.infn.it](mailto:camilla.didonato@na.infn.it) (C. Di Donato),  
[marek.jacewicz@physics.uu.se](mailto:marek.jacewicz@physics.uu.se) (M. Jacewicz).

## 1 Introduction

The Chiral Perturbation Theory (ChPT) provides an accurate description of interactions and decays of light mesons [1]. The Wess-Zumino-Witten (WZW) term in the ChPT Lagrangian accounts for anomalous decays involving an odd number of pseudoscalar mesons. The triangle anomaly is responsible for the two-photon decays of the  $\pi^0/\eta/\eta'$  mesons. Both triangle and box anomalies should contribute to the  $\eta^{(\prime)} \rightarrow \pi^+\pi^-\gamma$  decays. Since the kinematic region of the decays is far from the chiral limit, the amplitude of the  $\pi^+\pi^-$  final state interaction has to be properly included. The decays are therefore often described by a resonant contribution due to the  $\rho$ -meson exchange using the Vector Meson Dominance (VMD) model, and an additional contact term (CT), whose strength is constrained by the requirement to obtain a total contribution consistent with the WZW term in the chiral limit. In the case of  $\eta \rightarrow \pi^+\pi^-\gamma$  the resonant  $\rho$  contribution is sub-dominant, making the partial decay width sensitive to the CT, while for the  $\eta' \rightarrow \pi^+\pi^-\gamma$  decay the partial width is dominated by the resonance but the direct term will influence the shape of the di-pion invariant mass distribution. The present world average of the  $\eta \rightarrow \pi^+\pi^-\gamma$  partial width,  $\Gamma(\eta \rightarrow \pi^+\pi^-\gamma) = (60 \pm 4) \text{ eV}$  [2], provides strong evidence of the CT in the box anomaly when compared with the values obtained with and without the direct term,  $(56.3 \pm 1.7) \text{ eV}$  and  $(100.9 \pm 2.8) \text{ eV}$ , respectively [3].

Various approaches have been used to describe the final state interaction in these decays: the Hidden Local Symmetry (HLS) model [3], the chiral unitary approach [4] and the Omnes function encoding pion-pion interaction [5]. A model-independent approach, based on a combination of ChPT and dispersion theory, has been recently proposed, where a parametrisation of the experimental pion vector form factor is used instead of VMD [6].

Recently, CLEO [7] has measured the ratio  $R_\eta = \Gamma(\eta \rightarrow \pi^+\pi^-\gamma)/\Gamma(\eta \rightarrow \pi^+\pi^-\pi^0) = 0.175 \pm 0.007_{\text{stat}} \pm 0.006_{\text{syst}}$ , which differs by more than  $3\sigma$  from the average of previous measurements [8,9],  $R_\eta = 0.207 \pm 0.004$  [10]. We present a new measurement of  $R_\eta$  with smaller statistical and systematic errors, together with the fit of the  $M_{\pi\pi}$  distribution according to the model-independent approach presented in [6].

## 2 The KLOE detector at DAΦNE

The KLOE experiment operated at the Frascati  $\phi$ -factory, DAΦNE, an  $e^+e^-$  collider running at a center-of-mass energy of  $\sim 1020 \text{ MeV}$ , the mass of the  $\phi$  meson. The beams collide at a crossing angle of  $(\pi - 0.025) \text{ rad}$ , producing  $\phi$  mesons with a small momentum in the horizontal plane,  $p_\phi = 12.5 \text{ MeV}$ .

The detector consists of a large cylindrical Drift Chamber (DC), surrounded by a lead-scintillating fiber electromagnetic calorimeter (EMC) and a superconducting coil around the EMC providing a 0.52 T field. The DC [11], 4 m in diameter and 3.3 m long, has 12,582 all-stereo tungsten sense wires and 37,746 aluminum field wires. The chamber shell is made of carbon fiber-epoxy composite with an internal wall of 1.1 mm thickness, the gas used is a 90% helium, 10% isobutane mixture. The spatial resolutions are  $\sigma_{xy} \sim 150 \mu\text{m}$  and  $\sigma_z \sim 2 \text{ mm}$  and the momentum resolution is  $\sigma(p_\perp)/p_\perp \approx 0.4\%$ . The EMC [12] consists of a barrel and two endcaps, for a total of 88 modules, and covers 98% of the solid angle. The modules are read out at both ends by photomultipliers, both in amplitude and time. The readout granularity is  $\sim (4.4 \times 4.4) \text{ cm}^2$ , for a total of 2440 cells arranged in five layers. The energy deposits are obtained from the signal amplitude, while particle position along fiber direction is obtained from the arrival time difference of the signals to the photo-multipliers at the ends of each calorimeter cell. Signals of calorimeter cells close in time and space are grouped into clusters and the cluster energy  $E$  is the sum of the cell energies. The cluster time  $T$  and position  $\vec{R}$  are energy-weighted averages. Energy and time resolutions are,  $\sigma_E/E = 5.7\%/\sqrt{E \text{ (GeV)}}$ , and  $\sigma_t = 57 \text{ ps}/\sqrt{E \text{ (GeV)}} \oplus 100 \text{ ps}$ , respectively. The trigger [13] uses both calorimeter and chamber information. Data are then analysed by an event classification filter (EVCL), that organises data in different output files, according to their particle content [14].

### 3 Event selection

The analysis has been performed using  $558 \text{ pb}^{-1}$ , collected at  $\sqrt{s} \simeq 1020 \text{ MeV}$ , which correspond to about  $22 \times 10^6$   $\eta$ -mesons produced. KLOE Monte Carlo (MC) program [14] is used to simulate the final states produced in  $e^+e^-$  collisions, taking into account machine parameters and beam-related background on run-by-run basis. At KLOE, the  $\eta$  mesons are produced together with a monochromatic recoil photon,  $E_\gamma = 363 \text{ MeV}$ , through the radiative decay  $\phi \rightarrow \eta\gamma$ . The final state under study is  $\pi^+\pi^-\gamma\gamma$  with the main background coming from  $\phi \rightarrow \pi^+\pi^-\pi^0, \pi^0 \rightarrow \gamma\gamma$ . Another important background is  $\eta$  decay  $\phi \rightarrow \eta\gamma \rightarrow \pi^+\pi^-\pi^0\gamma \rightarrow \pi^+\pi^-3\gamma$  with one undetected photon. In the MC generator the signal is simulated using a matrix element

$$|M|^2 \simeq k^2 \sin^2 \theta \left( \frac{M_{\pi\pi}}{q} \right) \frac{\Gamma}{(M_\rho^2 - M_{\pi\pi}^2)^2 + M_\rho^2 \Gamma^2}$$

where,  $k$  is the photon momentum in the  $\eta$  rest frame,  $\theta$  is the angle between the  $\pi^+$  and the photon in the di-pion rest frame,  $q$  is the momentum of both pions in the di-pion rest frame and  $\Gamma = 124 \cdot (q/q_0)^3 \text{ MeV}$  with  $q_0$  being the value of  $q$  at  $\rho$ -meson resonance [8].

After the EVCL filter, a preselection is performed, requiring at least two tracks with opposite charge pointing to the interaction point (IP) and at least two clusters in time<sup>1</sup>, not associated to any track, having energy  $E_{clu} \geq 10$  MeV and a polar angle in the range  $(23^\circ - 157^\circ)$ . Tracks are sorted according to the distance of the point of closest approach from the IP. The first two tracks with opposite charge are selected as pion candidates.

### 3.1 $\eta \rightarrow \pi^+\pi^-\gamma$ selection

We require that the most energetic cluster has an energy  $E_{clu} > 250$  MeV and we identify it as the photon ( $\gamma_\phi$ ) recoiling against the  $\eta$  in the  $\phi \rightarrow \eta\gamma$  decay. Moreover, we ask that the  $\gamma_\phi$  is inside the calorimeter barrel (with a polar angle in the range  $55^\circ - 125^\circ$ ), to reject events with cluster split between barrel and endcap. To reject electrons, cuts on cluster-track association and identification by time of flight (TOF) are used. These cuts reject Bhabha scattering background and other processes with electrons in the final state. We exploit the  $\phi \rightarrow \eta\gamma$  decay kinematics, to evaluate the  $\gamma_\phi$  energy:

$$\vec{p}_\phi = \vec{p}_\eta + \vec{p}_{\gamma_\phi} \quad E_{\gamma_\phi} = \frac{M_\phi^2 - M_\eta^2}{2(E_\phi - |\vec{p}_\phi| \cos \vartheta)}$$

where,  $\vartheta$  is the angle between  $\gamma_\phi$  and the  $\phi$  meson momentum,  $\vec{p}_\phi$ , measured run by run with high accuracy using Bhabha scattering events. This allows us to improve the energy measurement accuracy of the recoil photon to 0.1%. Using  $\phi$  and  $\pi$ -mesons momenta, we determine the direction of the photon ( $\gamma_\eta$ ) from  $\eta$  decay:

$$\vec{p}_{\gamma_\eta} = \vec{p}_\phi - \vec{p}_{\pi^+} - \vec{p}_{\pi^-} - \vec{p}_{\gamma_\phi}$$

the  $\gamma_\eta$  photon direction is then compared with the direction of each neutral cluster:  $\Delta\varphi = \varphi_{clu} - \varphi_{\gamma_\eta}$  (here, and in the following, the angles are evaluated using variables in the transverse plane<sup>2</sup>). If no clusters with  $\Delta\varphi < 8.5^\circ$  are found, the event is rejected. The cluster with the minimum value of  $\Delta\varphi$  is identified with  $\gamma_\eta$ . In order to reject the  $\phi \rightarrow \pi^+\pi^-\pi^0$  background, the angle between the two photons in the  $\pi^0$  reference frame, evaluated using the  $\phi$  and the  $\pi$ -meson momenta, is calculated and it is required to be smaller than  $165^\circ$ . The  $\pi^+\pi^-\gamma$  mass spectrum is shown in Fig. 1. The candidate events are selected requiring  $539.5 \text{ MeV} < M_{\pi^+\pi^-\gamma} < 554.5 \text{ MeV}$ .

<sup>1</sup> We require for each cluster  $|T_{clu} - R_{clu}/c| < 5\sigma_{T_{clu}}$ , where  $T_{clu}$  is the arrival time at the EMC,  $R_{clu}$  is the distance of the cluster from the beam interaction point, and  $c$  is the speed of light.

<sup>2</sup> The azimuthal angle of the cluster is measured with an angular resolution of 6 mrad using the position of the calorimeter cell. The polar angle is instead determined by the time difference of the signals at each side of the barrel and is affected by larger uncertainty. The use of azimuthal angle reduces the systematics.

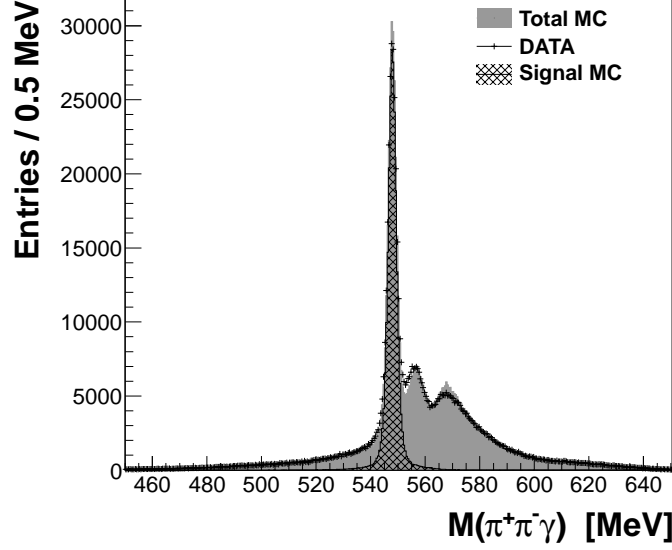


Fig. 1. The  $\pi^+\pi^-\gamma_\eta$  invariant mass distribution. Crosses are experimental points, the hashed area is the MC signal  $\eta \rightarrow \pi^+\pi^-\gamma$ , the filled region represents the total MC. Relevant background is due to  $\phi \rightarrow \pi^+\pi^-\pi^0$  events and much smaller contribution from  $\phi$ -meson decay into kaons for higher masses as well as  $\phi \rightarrow \eta\gamma$  events for the masses below the signal peak.

### 3.2 $\eta \rightarrow \pi^+\pi^-\pi^0$ selection

The process  $\phi \rightarrow \eta\gamma$  with  $\eta \rightarrow \pi^+\pi^-\pi^0$  represents a good control sample, having a topology similar to the signal. Moreover, in the ratio  $\Gamma(\eta \rightarrow \pi^+\pi^-\gamma)/\Gamma(\eta \rightarrow \pi^+\pi^-\pi^0)$  the luminosity, the  $\phi$  production cross section and the  $BR(\phi \rightarrow \eta\gamma)$  cancel out. We use the same preselection as for the  $\eta \rightarrow \pi^+\pi^-\gamma$  signal and calculate the missing four-momentum:

$$\mathbf{P}_{\text{miss}} = \mathbf{P}_\phi - \mathbf{P}_{\pi^+} - \mathbf{P}_{\pi^-} - \mathbf{P}_{\gamma_\phi}$$

where the variables in the formula represent the four-momenta of the  $\phi$  meson and of the decay products. For the  $\eta \rightarrow \pi^+\pi^-\pi^0$  sample, the missing mass peaks at the  $\pi^0$  mass value and we select events with  $|M_{\text{miss}} - M_{\pi^0}| < 15$  MeV. The remaining background is rejected by an angular cut applied to the two photons in the  $\pi^0$  rest frame,  $\varphi_{\gamma\gamma}^{3\pi} > 165^\circ$ . Figure 2 shows the distribution of the missing mass and  $\varphi_{\gamma\gamma}^{3\pi}$ . The two cuts select  $N(\eta \rightarrow \pi^+\pi^-\pi^0) = 1.116 \cdot 10^3$  events. The global selection efficiency is  $\varepsilon = 0.2276 \pm 0.0002$  with residual background contamination of 0.65%.

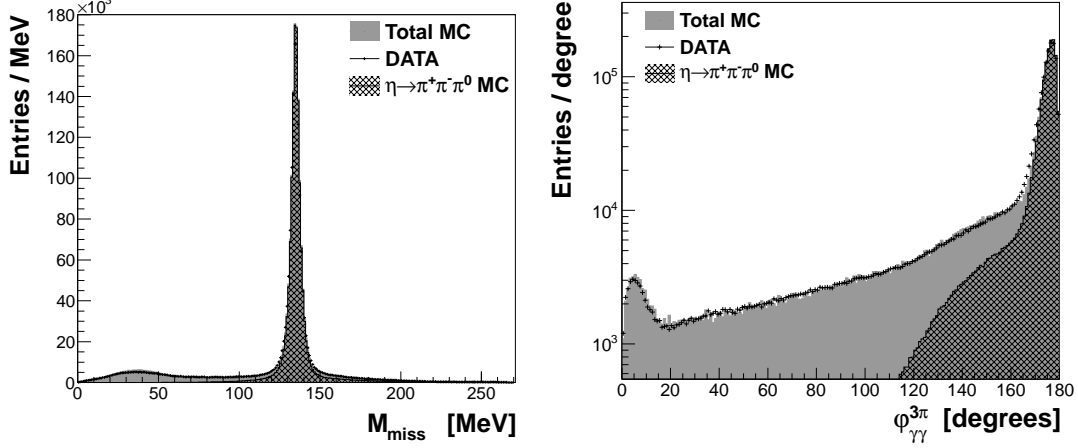


Fig. 2. Normalisation sample  $\eta \rightarrow \pi^+\pi^-\pi^0$ . Left -  $\pi^+\pi^-\gamma_\phi$  missing mass distribution. Right - event distribution for the angle between prompt neutral clusters in the  $\pi^0$  rest frame evaluated in the transverse plane,  $\varphi_{\gamma\gamma}^{3\pi}$ . Crosses are experimental points, the hashed area is the MC  $\eta \rightarrow \pi^+\pi^-\pi^0$ , the filled region represents the total MC, where the only relevant background contribution is due to  $\phi \rightarrow \pi^+\pi^-\pi^0$  events.

## 4 Results

### 4.1 The ratio $\Gamma(\eta \rightarrow \pi^+\pi^-\gamma)/\Gamma(\eta \rightarrow \pi^+\pi^-\pi^0)$

The total selection efficiency for the signal  $\eta \rightarrow \pi^+\pi^-\gamma$  is  $\varepsilon = 0.2131 \pm 0.0004$ . In the final sample, the relative weights of signal and background components are evaluated with a fit to the  $E_{\text{miss}} - P_{\text{miss}}$  distribution of the  $\pi^+\pi^-\gamma_\phi$  system, with the MC shapes of the remaining background and signal MC, Fig. 3. Signal events are counted in the range  $|E_{\text{miss}} - P_{\text{miss}}| < 10$  MeV. We find  $N(\eta \rightarrow \pi^+\pi^-\gamma) = 204950 \pm 497$  events, with a background contamination at level of 10%. The analysis has been repeated on an independent sample selected without EVCL filter to evaluate any bias due to the event classification. An overall correction factor is used to account for data/MC difference related to event classification:  $K_{EVCL} = \frac{\varepsilon_{\pi^+\pi^-\gamma}^{MC} \cdot \varepsilon_{\pi^+\pi^-\pi^0}^{data}}{\varepsilon_{\pi^+\pi^-\gamma}^{data} \cdot \varepsilon_{\pi^+\pi^-\pi^0}^{MC}} = 1.010 \pm 0.009$ .

Combining the results we obtain the ratio:

$$R_\eta = \frac{\Gamma(\eta \rightarrow \pi^+\pi^-\gamma)}{\Gamma(\eta \rightarrow \pi^+\pi^-\pi^0)} = 0.1856 \pm 0.0005_{\text{stat}} \pm 0.0028_{\text{syst}}$$

This result is in agreement with the recent CLEO measurement [7], while improving the accuracy of a factor better than three, thus confirming a smaller value for  $R_\eta$  with respect to previous evaluations [8,9].

The systematic uncertainties due to analysis cuts have been evaluated by

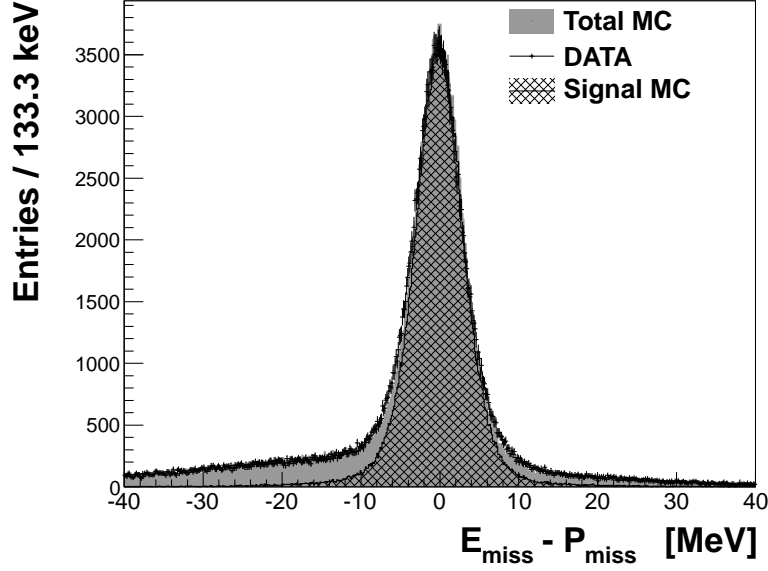


Fig. 3.  $E_{\text{miss}} - P_{\text{miss}}$  distribution for the  $\pi^+\pi^-\gamma\phi$ . The sample has been selected applying all the cuts described in Sec.3.1. The event counting is performed in the region  $|E_{\text{miss}} - P_{\text{miss}}| < 10$  MeV.

Source of Uncertainty	Cut Value	Window cut	Fractional Error on $R_\eta$
$\varphi_{\gamma\gamma}^{\pi^+\pi^-\gamma}$	$< 165^\circ$	$\pm 2^\circ$	$\pm 0.6\%$
$\Delta\varphi$	$< 8.5^\circ$	$\pm 2^\circ$	$\pm 0.4\%$
$ M_{\pi^+\pi^-\gamma} - M_\eta $	$< 7.5$ MeV	$\pm 2$ MeV	$\pm 0.6\%$
$E_{\text{min}}^\gamma$	$> 10$ MeV	$\pm 2$ MeV	$\pm 0.1\%$
$E_{\text{clu}}^{\gamma\phi}$	$> 250$ MeV	$\pm 4$ MeV	$\pm 0.1\%$
$ M_{\text{miss}} - M_{\pi^0} $	$< 15$ MeV	$\pm 4$ MeV	$\pm 0.4\%$
$\varphi_{\gamma\gamma}^{3\pi}$	$> 165^\circ$	$\pm 2^\circ$	$\pm 0.1\%$
EVCL			$\pm 0.9\%$
Fit $E_{\text{miss}} - P_{\text{miss}}$			$\pm 0.6\%$
Total			1.5%

Table 1

Summary table of systematic uncertainties on  $R_\eta$ .

varying the cuts and re-evaluating the value of  $R_\eta$ . Each cut is moved  $\pm 2\sigma$  with respect to the value used in the analysis, where  $\sigma$  is the resolution on the reconstructed variable. The corresponding error for each source of systematics is reported in Table 1. The total error is taken as the quadratic sum of all of the contributions.

#### 4.2 Fit to di-pion invariant mass

The  $M_{\pi\pi}$  dependence of the decay amplitude has been studied in several frameworks. The HLS model, in particular, has been investigated in [15] and more



recently in [3]. In this approach, the relative strength of the CT and the resonance contribution from VMD are fixed. The model-independent approach in [6], based on ChPT and dispersive analysis, does not fix this relative strength and parametrises the CT via a process-specific term. We use the last method to fit the di-pion invariant mass distribution. The function describing the partial width as a function of  $s_{\pi\pi} = M_{\pi\pi}^2$  is the following:

$$\frac{d\Gamma(\eta \rightarrow \pi^+\pi^-\gamma)}{ds_{\pi\pi}} = |AP(s_{\pi\pi})F_V(s_{\pi\pi})|^2 \Gamma_0(s_{\pi\pi}) \quad (1)$$

where,  $A$  is a normalisation factor and

$$\Gamma_0(s_{\pi\pi}) = \frac{1}{3 \cdot 2^{11} \cdot \pi^3 M_\eta^3} (M_\eta^2 - s_{\pi\pi})^3 s_{\pi\pi} \cdot \beta_\pi^3$$

is the simplest gauge-invariant matrix element multiplied by the phase-space term with  $\beta_\pi = \sqrt{1 - 4M_\pi^2/s_{\pi\pi}}$ .  $F_V(s_{\pi\pi})$  is the pion vector form factor, approximated in the energy range of interest by the polynomial  $|F_V(s_{\pi\pi})| = 1 + (2.12 \pm 0.01)s_{\pi\pi} + (2.13 \pm 0.01)s_{\pi\pi}^2 + (13.80 \pm 0.14)s_{\pi\pi}^3$ , where  $s_{\pi\pi}$  is expressed in  $\text{GeV}^2$  [6]. The  $P(s_{\pi\pi})$  function, a process-specific part, can be treated perturbatively in the frame of ChPT, for the decay of light mesons. Taylor expansion around  $s_{\pi\pi} = 0$  gives  $P(s_{\pi\pi}) = 1 + \alpha \cdot s_{\pi\pi} + \mathcal{O}(s_{\pi\pi}^2)$ . We fit the  $M_{\pi\pi}$  distribution by minimising the variable:

$$\chi^2 = \sum_i^{Nbin} \frac{(N_i^{data} - \sum_j^{Nbin} N_j^{Teo} \varepsilon_j S_{ij})^2}{\sigma_i^2} \quad (2)$$

where,  $N_i^{data}$  is the content of  $i$ -th bin after background subtraction,  $N_j^{Teo}$  is the content of  $j$ -th bin of the expected  $M_{\pi\pi}$  spectrum as from Eq.(1),  $\varepsilon_j$  is the efficiency,  $S_{ij}$  is the smearing matrix and  $\sigma_i^2 = \sigma_{N_i^{data}}^2 + \sigma_{N_i^{Teo}}^2$ , with  $\sigma_{N_i^{Teo}}^2 = \sum_j^{Nbin} (N_j^{Teo})^2 (\sigma_{\varepsilon_j}^2 S_{ij}^2 + \varepsilon_j^2 \sigma_{S_{ij}}^2)$ . Figure 4 shows the measured distribution compared with results of the fit taking into account efficiency and smearing.

Minimising the function in Eq. (2) we get

$$\alpha = (1.32 \pm 0.08_{\text{stat}} \pm 0.10_{\text{syst}} \pm 0.02_{\text{theo}}) \text{ GeV}^{-2}$$

with  $\chi^2/Ndf = 61/64$ . The theoretical error  $0.02 \text{ GeV}^{-2}$  accounts for uncertainty due to vector form factor parametrisation, and is determined mainly by the accuracy of the existing  $e^+e^- \rightarrow \pi^+\pi^-$  data. The fit is insensitive to the addition of a quadratic term in  $P(s_{\pi\pi})$ . The contributions to systematic uncertainty on  $\alpha$  are listed in Table 2. The value of  $\alpha$  is in agreement with the result of the WASA Collaboration obtained from the fit to the  $\gamma_\eta$  spectrum giving  $\alpha = (1.89 \pm 0.25_{\text{stat}} \pm 0.59_{\text{syst}} \pm 0.02_{\text{theo}}) \text{ GeV}^{-2}$  [16].

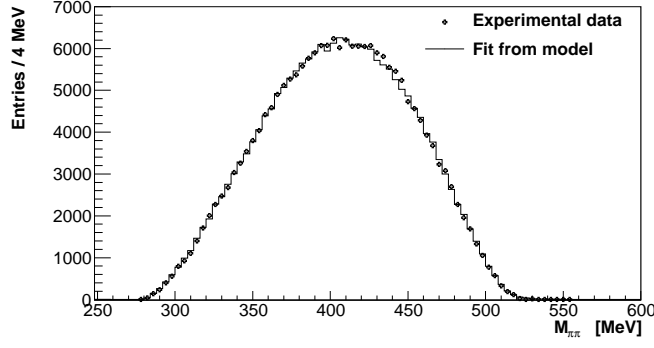


Fig. 4. Distribution of  $M_{\pi\pi}$  after background subtraction (black markers). Histogram is the fit of Eq. (1), corrected for acceptance and experimental resolution.

Source of Uncertainty	Cut Value	Window cut	$\Delta\alpha$ (GeV $^{-2}$ )
$\varphi_{\gamma\gamma}^{\pi^+\pi^-\gamma}$	$< 165^\circ$	$\pm 2^\circ$	$+0.07 / - 0.03$
$\Delta\varphi$	$< 8.5^\circ$	$\pm 2^\circ$	$+0.05 / - 0.06$
$ M_{\pi^+\pi^-\gamma} - M_\eta $	$< 7.5$ MeV	$\pm 2$ MeV	$+0.04 / - 0.04$
$E_{min}^\gamma$	$> 10$ MeV	$\pm 2$ MeV	$+0.01 / - 0.04$
Total			$+0.10 / - 0.9$

Table 2

Summary table of systematic uncertainties on  $\alpha$  parameter.

## 5 Conclusions

Using a data sample corresponding to an integrated luminosity of  $558 \text{ pb}^{-1}$ , we select about 205000  $\eta \rightarrow \pi^+\pi^-\gamma$  and 1116000  $\eta \rightarrow \pi^+\pi^-\pi^0$  events from the  $\phi \rightarrow \eta\gamma$  decays. We obtain the ratio of the partial widths:

$$\Gamma(\eta \rightarrow \pi^+\pi^-\gamma)/\Gamma(\eta \rightarrow \pi^+\pi^-\pi^0) = 0.1856 \pm 0.0005_{\text{stat}} \pm 0.0028_{\text{syst}}$$

in agreement with the most recent result from CLEO [7].

Combining our measurement with the world average value  $\Gamma(\eta \rightarrow \pi^+\pi^-\pi^0) = (295 \pm 16) \text{ eV}$  [2], we find  $\Gamma(\eta \rightarrow \pi^+\pi^-\gamma) = (54.7 \pm 3.1) \text{ eV}$ , which is in agreement with the value expected in the HLS context including the contact-term contribution [3].

We have measured the di-pion invariant mass distribution and performed a fit using the model-independent approach of Ref. [6]. The fit gives  $\alpha = (1.32 \pm 0.08_{\text{stat}}^{+0.10}_{-0.09\text{syst}} \pm 0.02_{\text{theo}}) \text{ GeV}^{-2}$ .

## Acknowledgments

We thank the DAΦNE team for their efforts in maintaining low background running conditions and their collaboration during all data taking. We want

to thank our technical staff: G.F. Fortugno and F. Sborzacchi for their dedication in ensuring efficient operation of the KLOE computing facilities; M. Anelli for his continuous attention to the gas system and detector safety; A. Balla, M. Gatta, G. Corradi and G. Papalino for electronics maintenance; M. Santoni, G. Paoluzzi and R. Rosellini for general detector support; C. Piscitelli for his help during major maintenance periods. This work was supported in part by the EU Integrated Infrastructure Initiative Hadron Physics Project under contract number RII3-CT- 2004-506078; by the European Commission under the 7th Framework Programme through the Research Infrastructures action of the Capacities Programme, Call: FP7-INFRASTRUCTURES-2008-1, Grant Agreement No. 227431; by the Polish National Science Centre through the Grants No. 0469/B/H03/2009/37, 0309/B/H03/2011/40, DEC-2011/03/N/ST2/02641, 2011/01/D/ST2/00748 and by the Foundation for Polish Science through the MPD programme and the project HOMING PLUS BIS/2011-4/3

## References

- [1] J. Gasser, H. Leutwyler, Nucl. Phys. B **250** (1985) 465.
- [2] J. Beringer et al. (Particle Data Group), Phys. Rev. D **86** (2012) 010001.
- [3] M. Benayoun et al., Eur. Phys. J. C **31** (2003) 525.
- [4] B. Borasoy, R. Nissler, Nucl. Phys. A **740** (2004) 362
- [5] E.P. Venugopal and B.R. Holstein, Phys. Rev. D **57** (1998) 4397
- [6] F. Stollenwerk et al., Phys. Lett. B **707** (2012) 184.
- [7] A. Lopez et al., CLEO Collaboration, Phys. Rev. Lett. **99** (2007) 122001.
- [8] M. Gormley et al., Phys. Rev. D **2** (1970) 501.
- [9] J. J. Thaler et al., Phys. Rev. D **7** (1973) 2569.
- [10] W.-M. Yao et al. (Particle Data Group), J. Phys. G **33** (2006) 1.
- [11] M. Adinolfi et al., KLOE Collaboration, Nucl. Inst. and Meth. A **488** (2002) 51.
- [12] M. Adinolfi et al., KLOE Collaboration, Nucl. Inst. and Meth. A **482** (2002) 364.
- [13] M. Adinolfi et al., KLOE Collaboration, Nucl. Inst. and Meth. A **492** (2002) 134.
- [14] F. Ambrosino et al., KLOE Collaboration, Nucl. Inst. and Meth. A **534** (2004) 403.

- [15] C. Picciotto, Phys. Rev. D **45** (1992) 1569.
- [16] P. Adlarson et al., WASA-at-COSY Collaboration, Phys. Lett. B **707** (2012) 243.